Electronic Supplimentary Information

A high rate and stable electrode of the Na3V2O2x(PO4)2F3-2x-rGO composite with cellulose binder for Sodium-ion batteries†

*P. Ramesh Kumar [a], Young Hwa Jung [b], Syed Abdul Ahad [a] and Do Kyung Kim [a]**

[a] Department of Materials Science and Engineering, Korea Advanced Institute of Science and Technology (KAIST), 291 Daehak-ro, Yuseong-gu, Daejeon 305-701, Republic of Korea
[b] Beamline Department, Pohang Accelerator Laboratory (PAL), Pohang 37673, Republic of Korea

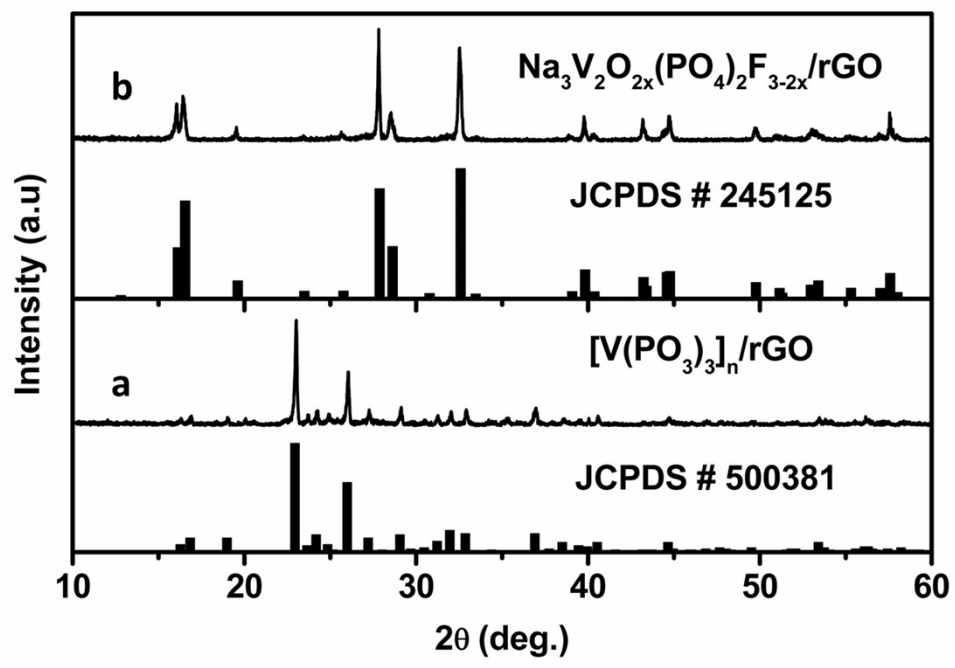

Figure S1: powder XRD patterns for the $[V(PO_3)_3]_x$-rGO and NVOPF-rGO composites along with their JCPDS data

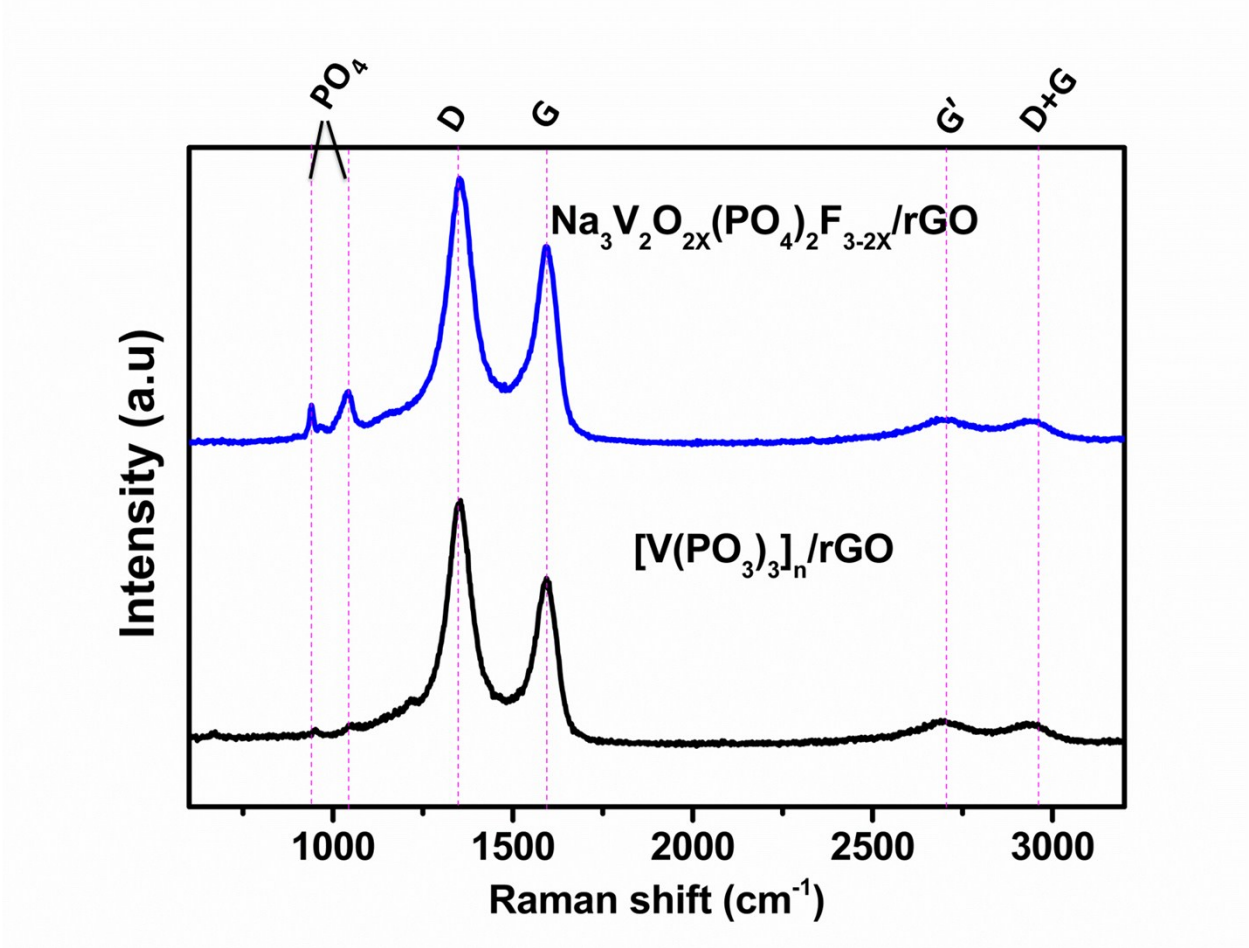

Figure S2: Raman spectra for both $[V(PO_3)_3]_n$-rGO and the $Na_3V_2O_{2x}(PO_4)_2F_{3-2x}$-rGO composites

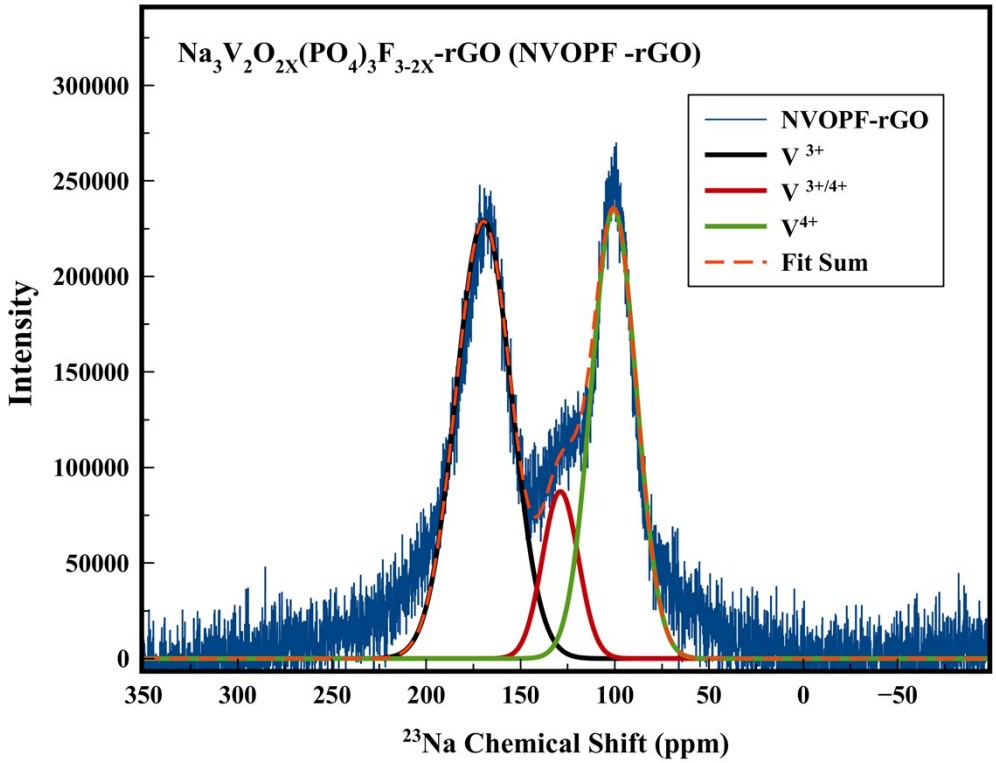

Figure S3: ^{23}Na solid-state NMR spectrum of the $Na_3V_2O_{2x}(PO_4)_2F_{3-2x}$-rGO composite

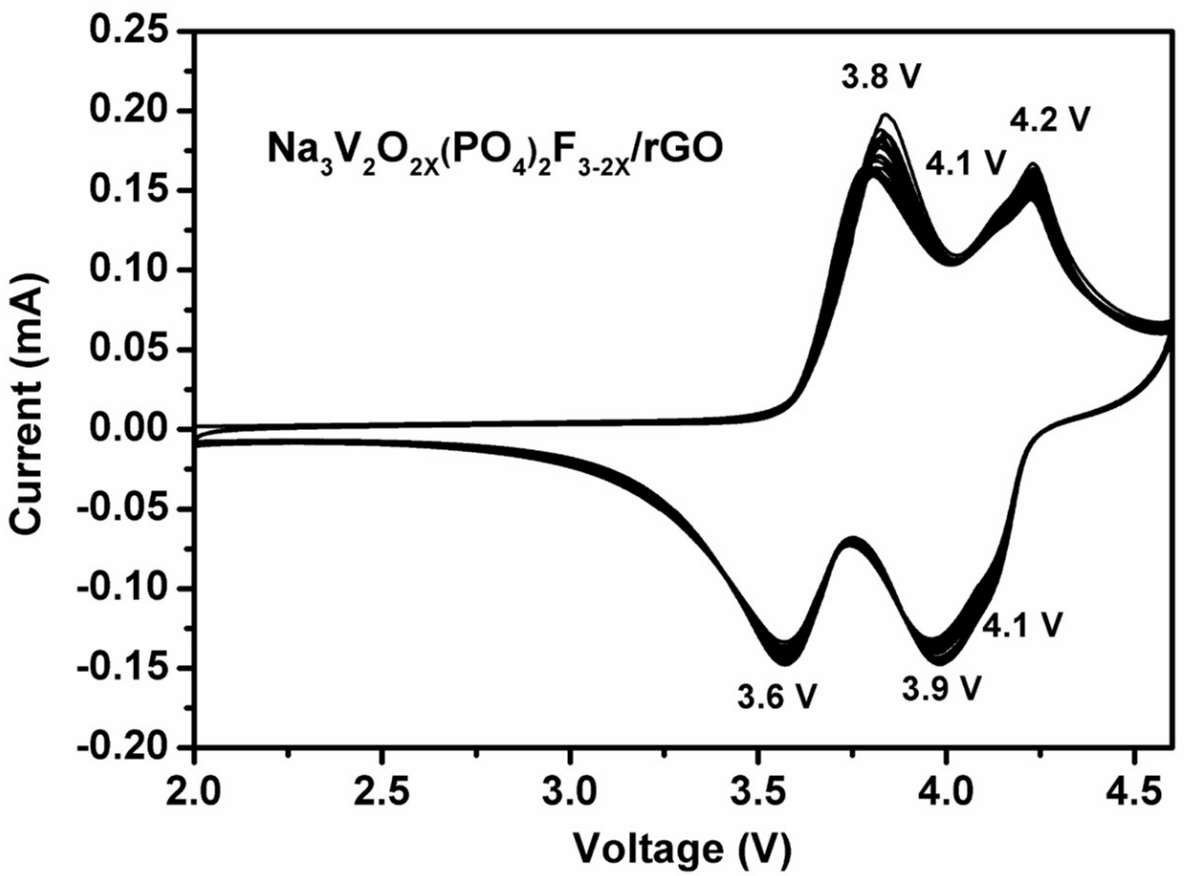

Figure S4: CV plot for the $Na_3V_2O_{2x}(PO_4)_2F_{3-2x}$/rGO composite with PVDF binder.

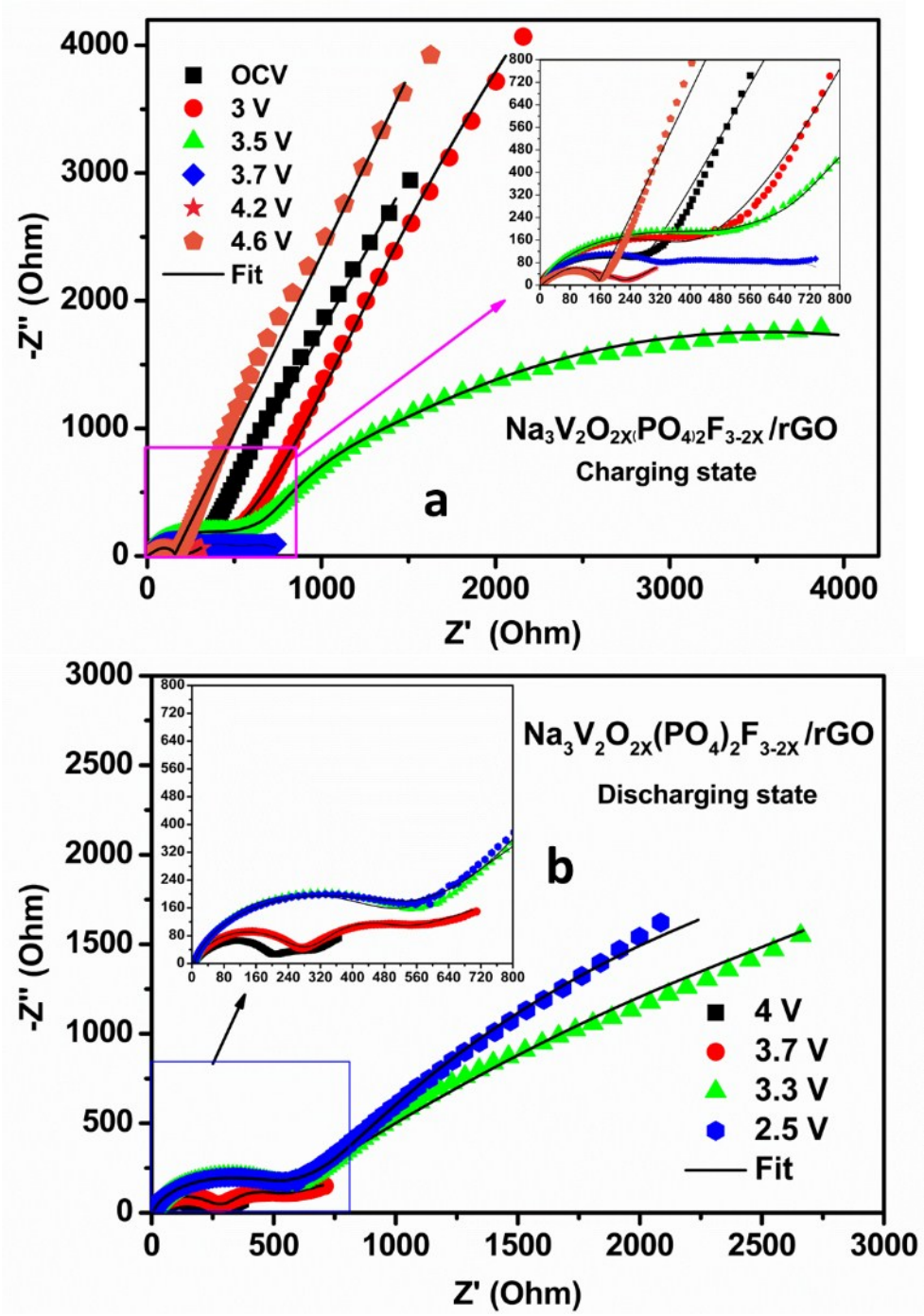

Figure S5: Nyquist plots for the $Na_3V_2O_{2x}(PO_4)_2F_{3-2x}$-rGO composite with CMC binder electrode during (a) charging and (b) discharging states.

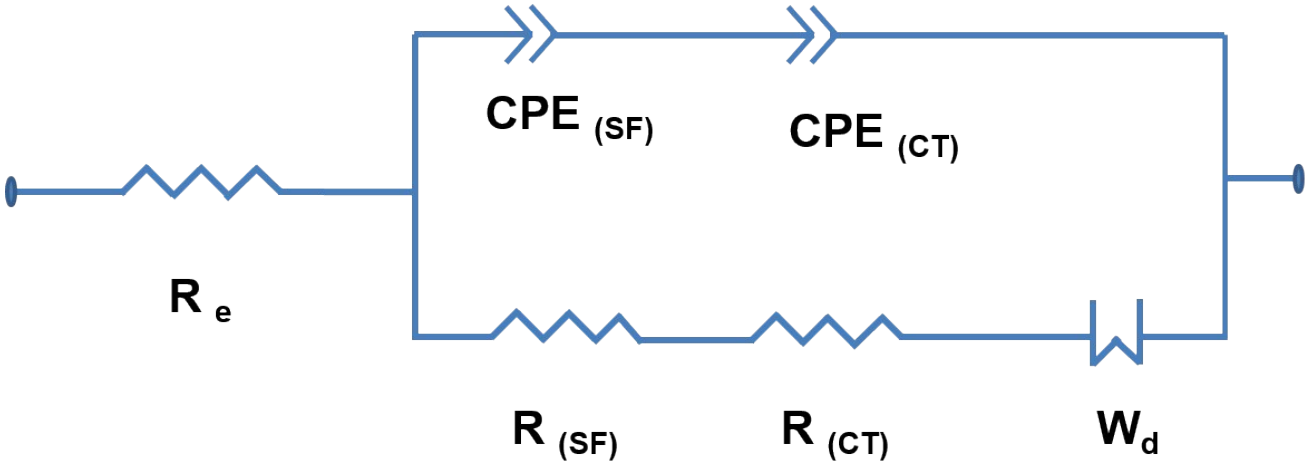

Figure S6: Electrical equivalent circuit consisting of resistors and constant phase elements for $Na_3V_2O_{2x}(PO_4)_2F_{3-2x}$/rGO composite electrode.

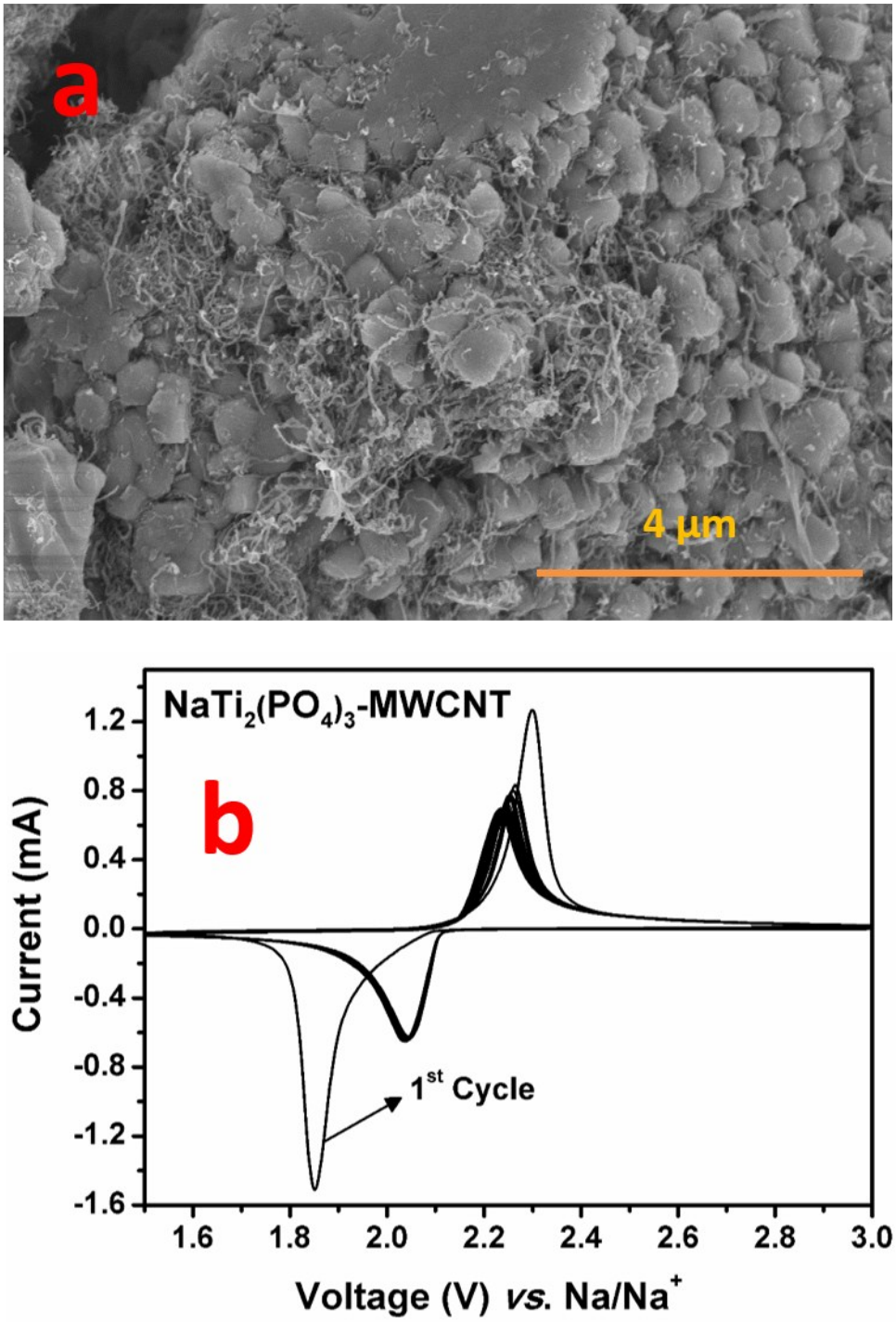

Figure S7: a) SEM image and b) Cyclic voltammetry plot of the $NaTi_2(PO_4)_3$-MWCNT versus Na/Na^+.